Aerodynamics of a Fixed Ground Plane for a Powered STOL Wind-Tunnel Model

J. E. Hackett* and J. L. Justice†
Lockheed-Georgia Company, Marietta, Ga.

Theoretical and experimental studies on a 0.10-scale C-130 STOL model, over a fixed ground plane, allowed a close examination both of ground boundary-layer effects and other aspects of such high-lift testing. Excellent experimental/theoretical agreement is demonstrated for both ground pressures (vortex-lattice techniques) and boundary-layer characteristics. Detailed prediction of ground boundary layers is shown to be feasible. Other aspects discussed include flow-breakdown criteria, contraction-lag effects, strut-fairing interference, and circulation around finite-chord ground planes.

Nomenclature

b = model span, ft
$\bar{c}$ = wing mean aerodynamic chord, ft
C_m = pitching moment coefficient, pitching moment/qSc
C_L = lift coefficient, lift/qS
C_{Lhb} = lift/qhb
C_p = static pressure coefficient
d = propeller diameter, ft
h = height of model above ground, ft
L = model lift, lbs.
S = model reference area, ft^2
q = wind-tunnel dynamic pressure, psf
T_c = thrust coefficient, thrust/eng./$2qd^2$
$V\infty$ = wind-tunnel mainstream velocity, fps
ρ = mass density of air, slugs/cu ft

1. Introduction

MOVING-belt ground simulation rigs are not universally popular, partly because of mechanical or reliability problems and installation time and cost, but also because adequate results are often thought to be possible without them. For existing tunnels built without an integral moving ground there is a choice between installing a fixed or a moving-ground plane, so boundaries of test validity for the fixed ground plane must be defined. Generalized experiments fail to give sufficiently detailed guidance because of the number of geometric variables involved. The present work combines theoretical vortex lattice techniques[1] with a three-dimensional boundary-layer calculation[2] on the ground plane to determine the conditions for separation, the increase in boundary-layer displacement thickness, and the decrease in skin friction as separation conditions are approached.

During the development of the theoretical methods, the opportunity arose for check comparisons against STOL/C-130 tests over a fixed ground plane.[3]

The fixed, finite-chord ground plane and test model, installed in the Lockheed-Georgia Low Speed Wind Tunnel, are shown in Figs. 1–3.

Ground-plane instrumentation included static pressure taps, Preston tubes (total pressure orifices resting against the wall calibrated in terms of skin friction at the wall),[4] and limited boundary-layer rakes. Some of this instrumentation is evident in Fig. 2.

The analyses include both takeoff and approach configurations. Takeoff flaps are designated as 25/0°, and approach flaps as 36/45° (36° on the fore flap with an additional 45°, relative to the fore flap, on the aft flap). The powered cases correspond to an approach flight condition. Figures 4 and 5 show lift curves, measured without and with propeller power applied, respectively, for takeoff and approach flap settings with and without the fixed ground plane installed. In powered cases with the ground plane installed at the minimum height, observations during the test showed that ground separation was evident at the higher incidences (denoted by solid symbols). In the unpowered case, identification of separation by means of tufts was uncertain, but Preston tube measurements on the centerline indicated the probable presence of separation, since skin friction approached zero (see Sec. 3). Figures 6 and 7 show the corresponding pitching moment curves. It is also apparent that the tail could induce ground boundary-layer separation, but this has not been investigated.

The lift results have been replotted in Figs. 8 and 9 for comparison with South's[5] and Turner's[6] criteria, respectively. South's result, which is based on floor tuft observations for a jet flapped wing configuration, fails to predict separation in the present case. Turner's criterion is based on deviations between fixed and moving ground results and may be shown to be the more conservative at aspect ratios above 6.67; consequently, it succeeds better for the present aspect ratio 10.07 model.

Though Turner's, South's, and the present work all involve powered models, it is possible that the impingement phenomenon is somewhat different quantitatively in the present case, because the deflected sheet is very much thicker. References 11 and 12 include a detailed discussion of powered model ground effects with a fixed and with a moving ground, together with recent experimental results.

Where impingement is absent, both criteria may be interpreted in terms of specific values of mean velocity deficit coefficients at the floor, caused by the bound vortex. This is equivalent to defining a floor boundary-layer separation criterion in terms of a specific value of pressure coefficient and ignoring both upstream history and lateral pressure gradients. Both are taken into account in the calculations discussed in Sec. 3.

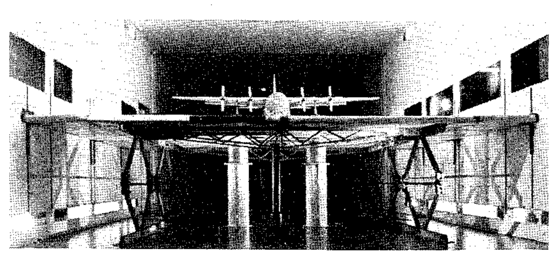

Fig. 1 Ground plane and model installed in Lockheed- Georgia low-speed wind tunnel.

Presented as paper 71-266 at the AIAA 6th Aerodynamic Testing Conference, Albuquerque, N. Mex., March 10–12, 1971; submitted September 1, 1972; revision received December 26, 1972.
Index category: Aircraft and Component Wind Tunnel Testing.

*Scientist. Member AIAA.
†Aerodynamics Engineer.

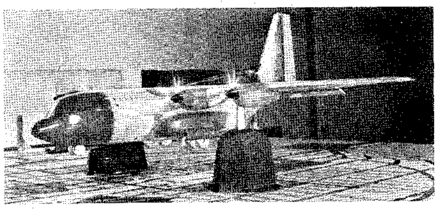

Fig. 2 Model installation—0.10 scale STOL/C-130-flap setting = 25/0° – h/b = 0.168.

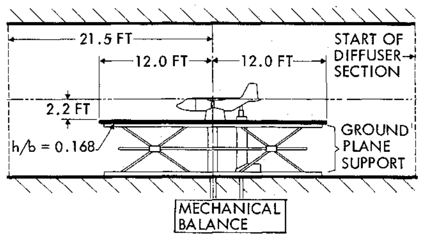

Fig. 3 Model/ground plane installation.

2. Potential-Flow Interference Effects

2.1 Circulation around the Ground Plane Itself

Before examining model-induced effects on the ground plane, it is appropriate to study the aerodynamics of the ground plane itself, which in the present case had finite chord. This is frequently the case in wind tunnels with a virtual center mechanical balance.

Joppa[7] has drawn attention to the "contraction lag" phenomenon, particularly its effect on rotors. This could also affect a finite-chord ground plane, if the leading edge were too close to the test-section entrance. For the tests described here, the second of a tandem pair of test sections was used. This section follows a contraction, from the larger test section, with an area ratio of 2:1, which occurs mainly in the vertical plane and which has gentle curvature at the downstream end. Sample calculations of flow angularity associated with the contraction-lag effect were made using the vortex-lattice model shown in Fig. 10. A maximum of ¼° angularity was evident at the test section entry, but at the position of the ground plane leading edge, 9.5 ft further downstream, the calculated cross-flow angles were negligible. The effect would be more pronounced for wind tunnels with higher contraction ratios.

Interference due to the use of a finite-chord ground plane was found to be significant. In the longitudinal plane of symmetry, for example, the model induces upwash at the ground plane leading edge and a stronger, predominantly trailing-vortex-induced downflow at the trailing edge. This gives rise to positive circulation which reduces the download on the ground to a value less than the lift on the model. In consequence, the ground effect experienced by the model is less than it should be.

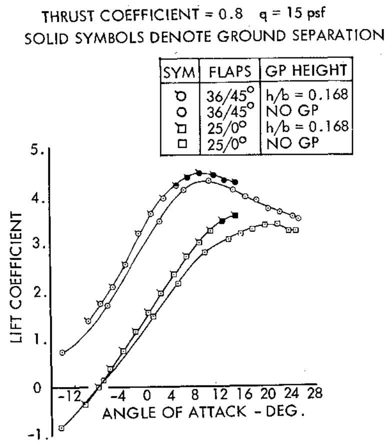

Fig. 5 Lifting characteristics of Lockheed STOL/C-130.

To quantify this, a vortex-lattice, lifting-surface theoretical model was studied having an aspect ratio 12 rectangular wing, situated one chord above a representative finite-chord ground plane. Datum calculations were performed for free air and for an infinite ground. On the finite ground, the total download was 20% less than the wing lift: the two are equal, but opposite in sense, for an infinite ground. As a result of the reduced finite-ground download, there was a 19% reduction in the ground-induced increment of wing lift, relative to the infinite-ground value. The effect was particularly marked near the wing root but less noticeable towards the tip.

Experimentally, these spurious circulation effects are more readily detected as a pressure rise on the underside of the ground plane, shown in Fig. 11. As model lift is increased, increased underside pressures become evident. These are associated with induced camber and induced incidence at the ground plane, which appear in unknown portions and which change sign in the spanwise direction outside the trailing vortices. It is probably conservative to consider the under-surface pressure rise as camber-related (the shape of the distribution in Fig. 11 certainly suggests this) and to make the linear assumption that there will be a corresponding equal pressure decrease on the upper surface. The upper surface pressures on the ground plane for the case illustrated would thus be 0.05–0.10 lower in C_p, depending upon model total lift, than if an infinite ground had been present.

In addition to the above potential flow effects, there was also considerable blockage below the ground plane caused by stiffeners, unfaired balance struts, etc. This undoubtedly influenced the ground plane circulation. As model incidence increased towards the stall, ground-plane under-surface pressures tended to stabilize, probably be-

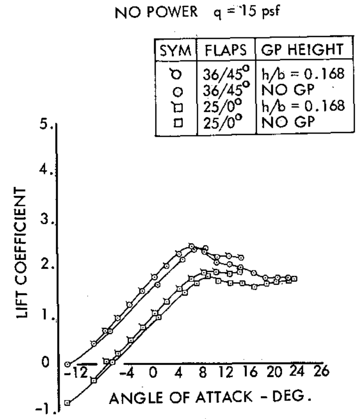

Fig. 4 Lifting characteristics of Lockheed STOL/C-130.

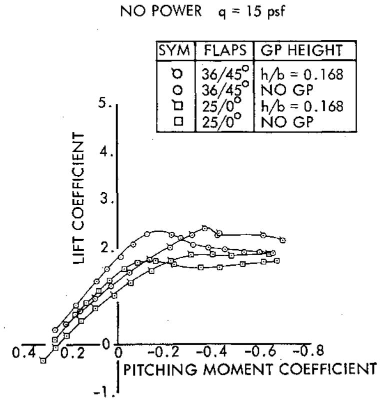

Fig. 6 Pitching moment characteristics of Lockheed STOL/C-130.

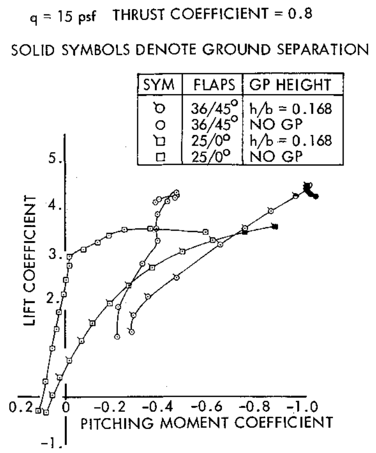

Fig. 7 Pitching moment characteristics of Lockheed STOL/C-130.

cause of increased blockage above the ground caused by the increased model cross section and stalled wakes.

It is sometimes suggested that unwanted positive circulation about a finite ground may be eliminated by the use of an uprigged trailing edge flap on the ground board. This seems appropriate, but for several reasons such an approach is impractical. For example, spanwise tailoring is probably necessary, dependent upon the model under test; it is not obvious how this should be determined. Even assuming a properly tailored flap chord, the flap angle should be adjusted in proportion to model lift, which is operationally inconvenient. Finally, the desired change in ground board camber is smooth and has approximately circular arc form; that for the aft flap is much too concentrated and also produces an unwanted leading edge suction peak. For these reasons, the use of a trailing edge flap on a finite-chord groundboard is not recommended.

2.2 Effects of the Wing-Support Strut Fairings

A theoretical, three-dimensional, vortex-lattice model was constructed, as illustrated in Fig. 12, which included model details and support-strut fairings. Predicted lift values agreed well with measurements for the linear part of the $C_L \sim \alpha$ curve. The effects of ground proximity on span-load distribution are shown in Fig. 13.

Figures 14 and 15 show outward loads on the strut fairings, which are induced by the spanwise outflow beneath the wing. The trailing vortex sheet from the top of the strut fairing induces upload on the inner part and download on the outer part of the wing. Although quite small in comparison with total load, these are not small in comparison with ground-induced load. It would be appropriate to "toe-in" the strut fairings by an amount dependent on wing lift. Figure 16 illustrates some typical calculated toe-in values which would tend to minimize the interference

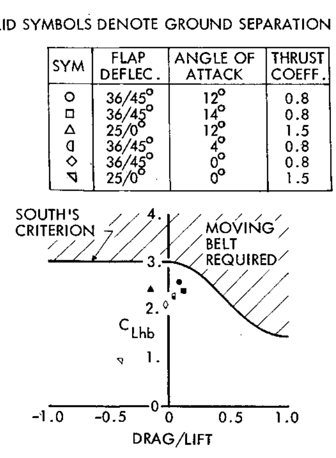

Fig. 8 Measured flow breakdown compared with South's criterion.

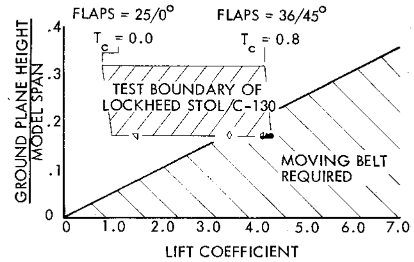

Fig. 9 Operational envelope of present results compared with Turner's criterion for moving ground requirement.

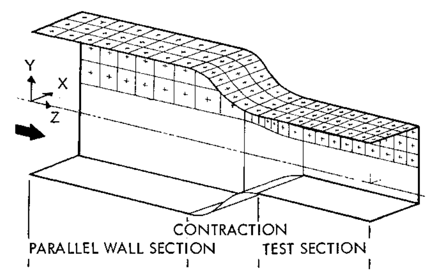

Fig. 10 Vortex lattice representation of wind tunnel.

at the wing. Comparison between the two halves of Fig. 17 reveals the calculated effects, at the surface of the ground plane, of adding strut fairings set at zero toe-in. Evidently, there are not only locally increased static pressures, associated with the leading edge stagnation at the base of each fairing, but also a general increase in the adverse static pressure gradient along the ground-plane centerline. Adverse effects on the ground boundary layer can be expected, which have more serious consequences at the wing than the direct strut-on-wing interference.

2.3 Pressure Distribution on the Ground Plane Upper Surface

Circulation values for the vortex lattice model of Fig. 12 were calculated for an infinite-ground condition together with pressures at the ground surface for use later in the three-dimensional boundary-layer calculations. The left-hand half of Fig. 18 is for a zero incidence, takeoff configuration and lift-induced effects are mild. Adding 12° incidence removed the small pressure peak near the front of the fuselage but intensified the strut fairing and wing lift-induced positive pressures. Though the predictions of Fig. 18 agree well with the measured pressures in Fig. 19 at zero incidence, a deeper examination is required at 12°. Allowances must be included for noticeable pressure coefficients which were found with the model removed. The comparison should also be made in the linear lift range.

In a limited study made in 1972, experimental ground pressures were corrected for model-absent effects using an appropriate velocity superposition technique. For 8° inci-

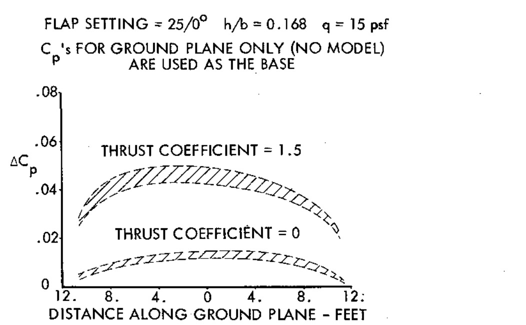

Fig. 11 Measured model effects on ground plane lower surface static pressure distribution.

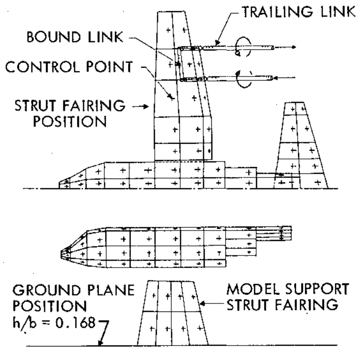

Fig. 12 Vortex lattice representation of Lockheed STOL/C-130.

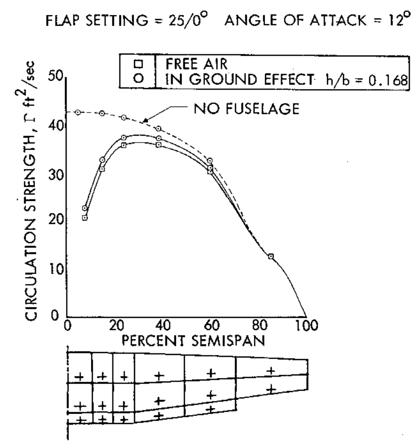

Fig. 13 Ground effect on wing loading of Lockheed STOL/C-130.

dence this moved the main positive pressure peak aft and reduced its intensity. Comparison with the corresponding theoretical prediction for an infinite ground then showed that the experimental peak was about 0.05 lower in C_p than the theoretical one, which is attributable to finite-ground effects. This agrees quite well with the predictions of Section 2.1, particularly bearing in mind that the 20% change mentioned there combines upper- and lower-surface effects. Boundary-layer displacement effects also modify the measured pressures.

3. The Ground Plane Boundary Layer: Unpowered Model

Calculated static pressure distributions, at the ground, were used in predicting the turbulent boundary-layer development. A computer program by Nash[2] was used which incorporates the shear stress model of Bradshaw[8] to represent the main features of turbulent energy transport. The method has been uniquely successful in previous comparisons with experimental measurements.[9]

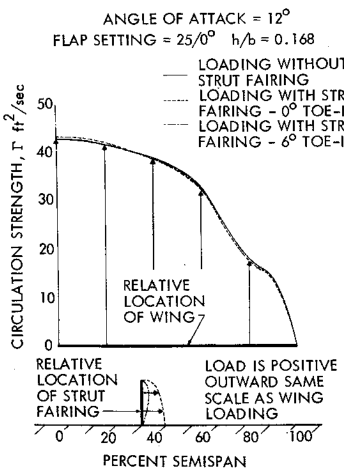

Fig. 14 Strut fairing interference on wing load distribution.

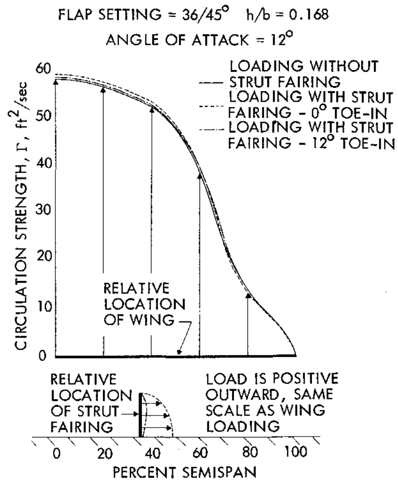

Fig. 15 Strut fairing interference on wind load distribution.

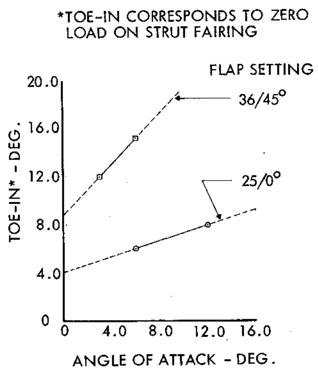

Fig. 16 Variation of strut fairing toe-in with wing angle of attack.

Figure 20 shows contours of boundary-layer thickness calculated using the predicted pressure distribution of Fig. 18. Thickness of the order of 3 in. are predicted beneath the model. The minimum clearance, at 12° incidence, between the aft fuselage and the ground plane is about $7\frac{1}{2}$ in. The only experimental boundary-layer measurements available for comparison are Preston tube readings on the ground plane centerline. Good agreement is evident in Fig. 21, particularly considering that the only experimental input to the theoretical line concerns upstream boundary-layer starting details. Improved agreement could be expected if the lower, measured static pressures of Fig. 19 were used.

Displacement effects of the ground boundary layer, some 27-in. below the wing, have also been investigated. At the relatively modest C_L values of Figs. 20 and 21, the

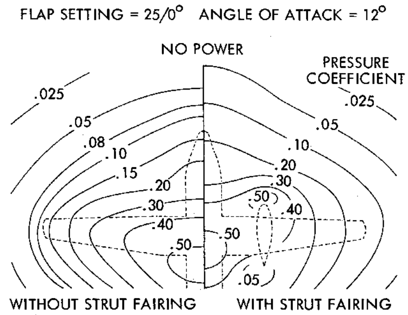

Fig. 17 Predicted static pressure distribution on the ground plane: strut fairing effect.

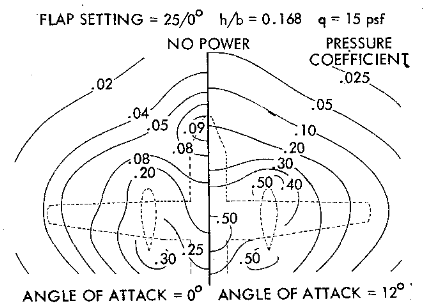

Fig. 18 Predicted static pressure distribution on the ground plane: incidence effect.

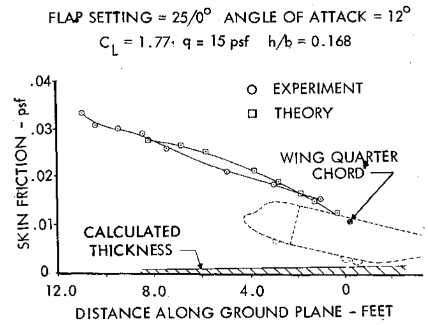

Fig. 21 Properties of the ground plane boundary layer during Lockheed STOL/C-130 tests.

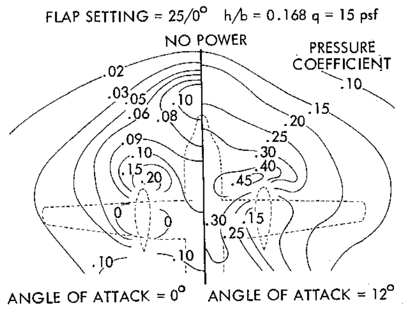

Fig. 19 Measured static pressure distribution on ground plane.

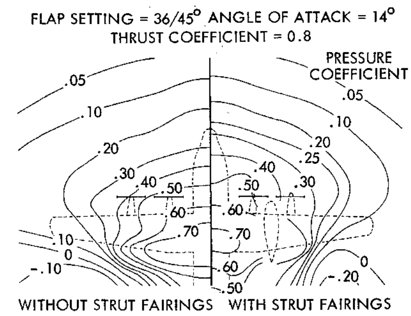

Fig. 22 Measured static pressure distribution on the ground plane.

boundary-layer total thickness is about 3 in., but the corresponding displacement thickness is too small for either incidence or super-velocity effects at the wing to be very significant. The results of the simplified calculations which were presented in the conference version of this paper were in error because they failed to include boundary-layer displacement effects downstream of the wing. Recent studies, extending the boundary-layer calculations further downstream, have shown that the boundary-layer displacement surface "hump" can possess a surprising degree of fore-aft symmetry, which corresponds to the symmetry in the pressure field. (See also Ref. 11). This low-Reynolds number phenomenon causes positive wing incidence effects induced by the forward boundary-layer displacement surface to be substantially cancelled out by negative incidence, induced by the aft part of that surface. To examine this further, a simplified example was run with the same wing height but with C_{Lhb} artificially increased to 95% of the floor separation value. The forward boundary layer induced almost 2° positive incidence at the wing but, at the low Reynolds number of the example, cancellation by the aft part reduced the net effect to minus 0.13°. This was accompanied by a 2.7% supervelocity at the quarter chord of the wing.

At higher Reynolds numbers the negative-incidence-inducing, boundary-layer thinning aft of the positive pressure hump becomes much more marked than in the above example. The detailed effects at the model are the subject of a continuing investigation.[11,12]

Probably the most significant aspect of the symmetry in the ground boundary-layer displacement surface, discussed above, arises when separation occurs. If separation does occur, several degrees of upwash may be induced by the forward boundary layer, no longer balanced by aft symmetry, in addition to any effect the separation surface itself may have.

4. Power Effects

Potential-flow theoretical methods were not available to handle powered cases. However, skin-friction measurements still permit quantitative evaluation of boundary-layer behavior. The more than doubled positive pressure coefficients evident in comparing Fig. 22 with Fig. 19 reflect an increase in lift coefficient from 1.9 to 4.3 when power and additional flap are present. As might be expected from positive C_p of 0.7, Fig. 22 corresponds to a separated flow condition below the model. This is confirmed in Fig. 23, in which measured centerline skin friction is shown to drop to zero just before the wing plane, and by the smoke-flow visualization in Fig. 24. It is recommended that the Preston tube instrumentation be installed to beyond the tail position.

5. Conclusions

Experiments on a 0.10-scale powered STOL/C-130 wind-tunnel model, mounted above an instrumented fixed

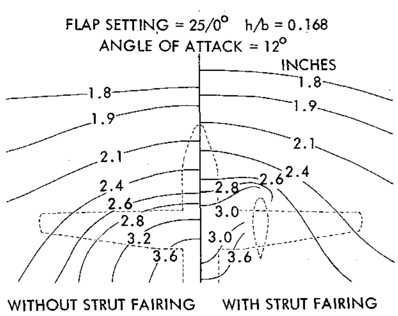

Fig. 20 Predicted boundary-layer thickness on the ground plane.

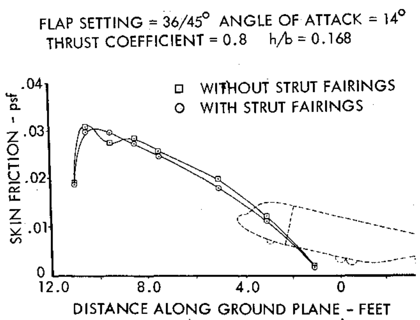

Fig. 23 Measured skin friction along ground plane centerline.

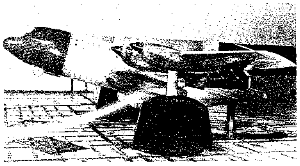

Fig. 24 Flow visualization smoke stream.

ground plane, have been critically scrutinized both experimentally and theoretically. Additional instrumentation included pressure taps, tufts, and skin-friction sensors at the ground. The theoretical approach comprised a vortex-lattice treatment for the potential flow, allied with a three-dimensional boundary-layer calculation for determination of boundary-layer displacement contours and skin friction.

Circulation around the Ground Plane

Since the ground plane was of the finite-chord type, checks were made to detect spurious tunnel- or model-induced circulation around it. Calculations showed that contraction was far enough upstream of the ground plane leading edge for contraction lag to be no problem. However, pressure measurements underneath the ground plane showed lift-dependent pressure increases, ΔC_p of up to 0.1, implying a reduced flow below and an increased flow above the ground plane. Though ground-plane trailing edge flaps have been used in the past in an attempt to rebalance the upper and lower flows, their camber is both abrupt and wrongly positioned and so cannot approximate very closely the desired, smooth distribution. Such flaps also need adjustment proportional to model lift, leading to awkward operational problems.

Strut Fairings

The underwing support-strut fairings were set at zero toe-in and experienced strong outward loads. Though the direct effect at the model is noticeable only at high lifts, the adverse indirect effects, associated with fixed ground boundary-layer separation, may become serious at quite low-lift levels. For this reason, it is recommended that strut toe-in be applied proportionally to model lift. The toe-in setting is probably most conveniently accomplished by equalizing the pressures sensed by symmetrically placed orifices on each side of the fairing. Some trial calculations showed that at least 20° of toe-in may be needed.

The Ground Plane Static Pressure and Boundary Layer

Excellent agreement was obtained at low angles of attack between predicted and measured ground-plane static pressure distributions. Use of the predicted pressures in a three-dimensional turbulent boundary-layer program produced good agreement with limited skin-friction measurements made along the ground plane centerline.

Theoretical pressure distribution and boundary-layer calculations were made for 25° flap with 12° incidence. This gave a lift coefficient of 1.9 and a total boundary-layer thickness of about three inches. There was good agreement between calculated and measured values of skin friction on the ground below the model centerline.

At higher, powered, lift coefficients it appears that penetration of the ground boundary layer by the fuselage and the occurrence of ground boundary-layer separation pose more of a hazard than does flow distortion by the boundary-layer displacement surface. Limited studies showed that the latter may become more important at high Reynolds numbers.

The prevention of boundary-layer impingement on the model and the suppression of fixed ground separation both provide a major reason for adopting a moving ground belt. However, the possible use of carefully-applied boundary-layer control appears to be feasible.[11,12]

The use of Preston (skin-friction measuring) tubes along the fixed ground-plane centerline is strongly recommended. They should extend from an upstream ground plane position to beyond the model tail.

References

[1]Hackett, J. E. and Praytor, E. B., "Vortex Roll-Up Behind High-Lift Wings," R&M ER-10406-2, Jan. 1970, Lockheed-Georgia Co., Marietta, Ga.

[2]Nash, J. F., "The Calculation of Three-Dimensional Turbulent Boundary Layer in Incompressible Flow," *Journal of Fluid Mechanics,* July 1969, Vol. 37, Pt. 4, pp. 625–642.

[3]Justice, J. L., "Data Memorandum for Test LSWT 059-STOL/C-130 in Ground Effect," June 1970, Lockheed-Georgia Co., Marietta, Ga.

[4]Patel, V. C., "Calibration of the Preston Tube and Limitations on Its Use in Pressure Gradients," *Journal of Fluid Mechanics,* 1965, Vol. 23, Pt. 1, pp. 185–208.

[5]South, P., "Measurements of Flow Breakdown in Rectangular Wind Tunnel Working Sections," LR-513, 1968, National Aeronautical Establishment, Canada.

[6]Turner, T. R., "A Moving-Belt Ground Plane for Wind-Tunnel Ground Simulation and Results for Two Jet-Flap Configurations," TN D-4228, 1967, NASA.

[7]Shindo, S. and Joppa, R. G., "The Effect of the Converging Flow Field of a Tandem-Test-Section on Longitudinal Stability Measurements," CR-1198, 1968, NASA.

[8]Bradshaw, P., Ferris, D. H., and Atwell, N. P., "Calculation of Boundary-Layer Development Using the Turbulent Energy Equation," *Journal of Fluid Mechanics,* 1967, Vol. 28, pp. 593–616.

[9]Nash, J. F., "An Explicit Scheme for the Calculation of Turbulent Boundary Layers," ASME Paper 71-FE-19, May 1971, Pittsburgh, Pa.

[10]"Low-Speed Wind Tunnel User Manual," ER-11000, 1970, Lockheed-Georgia Co., Marietta, Ga.

[11]Hackett, J. E. and Praytor, E. B., "Ground Effect and V/STOL Aircraft Configurations and its Simulation in the Wind Tunnel, Part I Introduction and Theoretical Studies," CR 114,495, 1972, NASA.

[12]Hackett, J. E., Boles, R. A., and Praytor, E. B., "Ground Effect for V/STOL Aircraft Configurations and its Simulation in the Wind Tunnel, Part II: Experimental Studies," CR 114,496, 1972, NASA.